



CRITICAL AXIAL LOADS FOR TRANSVERSELY LOADED MASONRY WALLS

A. E. Schultz¹ and N. J. Ojard² and H. K. Stolarski³

Abstract

The buckling behavior of unreinforced masonry (URM) walls subjected to out-of-plane lateral loads is described including numerical solutions for critical axial load capacity. The influence of bending on buckling strength is illustrated, and the strongly nonlinear interaction between critical load and out-of-plane bending is discussed. An experimental investigation and preliminary results on the stability of slender masonry walls are outlined, including combined lateral load-axial compression tests of URM specimens.

Key words: buckling, design formulas, load tests, out-of-plane bending, post-tensioned masonry, stability, transverse Loads, unreinforced masonry.

¹Arturo E. Schultz, Associate Professor, Department of Civil Engineering, University of Minnesota, Minneapolis, MN, 55455, schul088@tc.umn.edu

²Nels J. Ojard, Graduate Research Assistant, Department of Civil Engineering, University of Minnesota, Minneapolis, MN 55455, ojar0006@tc.umn.edu

³Henryk K. Stolarski, Professor, Department of Civil Engineering, University of Minnesota, Minneapolis, MN, 55455, stola001@tc.umn.edu

INTRODUCTION

Bending arising from out-of-plane lateral loads has a dramatic impact on the stability of URM walls (Fig. 1). Flexural tension stresses crack masonry and reduce the effective cross-section depth. This effect augments lateral deflection due to out-of-plane bending and gives rise to second-order ($P-\Delta$) moments. The additional bending generates more tension, which further reduces the cross-section, and can lead to instability (i.e. buckling).

Out-of-plane bending due to axial load eccentricity has been recognized to affect the stability of URM compression members (Angervo 1954, Sahlin 1961, Yokel 1971, Colville 1979). Previous research led to the development of design provisions that include eccentricity in the buckling capacity of URM walls. In the U.S., a check on the buckling strength of URM walls including the effects of axial load eccentricity is required (MSJC 1999). However, current code provisions do not address the effect of bending from out-of-plane loading on the stability of URM compression members.

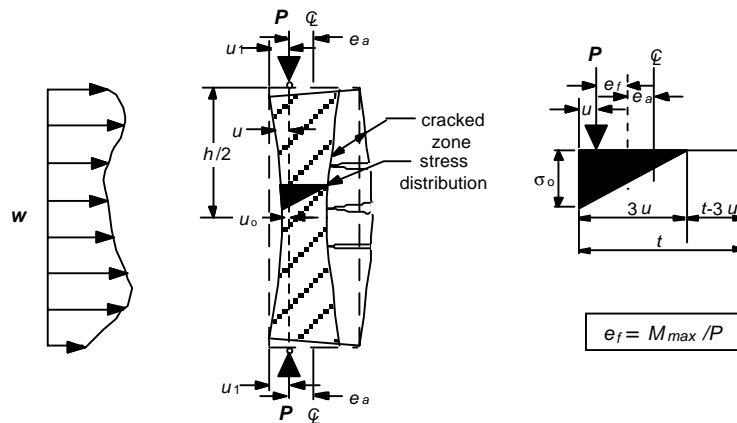


Fig. 1 Influence of lateral load on buckling of URM walls

Widespread problems in the performance of URM walls have not materialized in the U.S. in part because the existing URM building stock was designed according to older codes that are overly conservative. Yet, severe lateral loading events such as earthquakes, hurricanes and tornadoes often generate out-of-plane collapses of URM walls, and these failures are usually attributed to low tensile strength without proper attention given to stability concerns. However, new masonry construction often features members that are more slender and more highly stressed than those in older buildings, making stability concerns more important. And, these trends come at a time when design standards (*Minimum* 1998) and model codes (*NEHRP* 1998) have adopted significant increases in wind and seismic loads.

Previous Research

Linear analysis techniques have been used to solve the governing equation for the lateral deflection of URM walls under eccentric axial load (Angervo 1954, Sahlin 1961). In

these studies, computed deflections, as a function of axial load, were used to define critical loads. Solutions for the eccentric buckling strength of URM compression members have been developed in the U.S. (Yokel 1971, Colville 1979). Yokel illustrated the accuracy of this approach for prediction of the buckling strength of eccentrically loaded walls tested over a wide range of variables (1971).

The impact of masonry stress-strain nonlinearity on the buckling capacity of laterally-loaded URM walls has been studied recently (Romano 1993, La Mendola 1995, Ganduscio 1997). These researchers obtained analytical solutions for critical axial load which require iterative solutions of coupled, nonlinear equations. However, these solutions have not found their way to design practice due to their complexity. Sahlin (1961) had earlier considered the influence of out-of-plane bending on the buckling capacity of solid walls, but practical buckling solutions were not developed.

Influence of Bending on Critical Axial Loads

Yokel's formulation for the deflection of a linear, elastic URM wall, with solid cross-section and no tensile strength has been extended to include out-of-plane bending (Schultz et al. 2000). An additional flexural eccentricity e_f was defined as the ratio of bending moment M to axial load P (Fig. 1). Differential equations were derived for moment distributions arising from four combinations of support conditions and lateral load, including 1) equal end-moments on a simply-supported wall, 2) uniformly distributed lateral load on a simply-supported wall, 3) concentrated lateral load on top of a cantilever wall, and 4) uniformly-distributed lateral load on a cantilever wall.

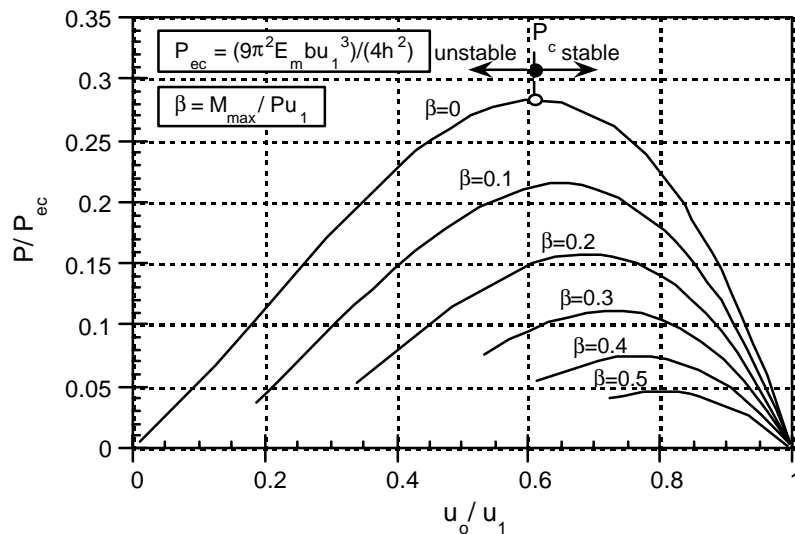


Fig. 2 Stability curves for simply-supported, uniformly loaded wall

Numerical solutions were obtained for the lateral displacement u of URM compression members under axial load (Fig. 1). These solutions describe load-displacement relationships like that shown in Fig. 2 for a simply-supported wall with a uniform load

w_u , and out-of-plane moment, as indicated by the parameter β , is seen to have a large influence on load-deflection behavior. Relative maxima represent points of impending instability, and the corresponding critical axial loads are the buckling strengths P_c .

For each of the four load cases considered, the ratios of critical load P_c to the equivalent critical load P_{ec} were correlated with the bending parameter β (Fig. 3), and a third-order polynomial with respect to β was fitted through this data. The numerical solutions, shown as discrete points in Fig. 3, are seen to be approximated closely by the polynomials, shown as solid lines.

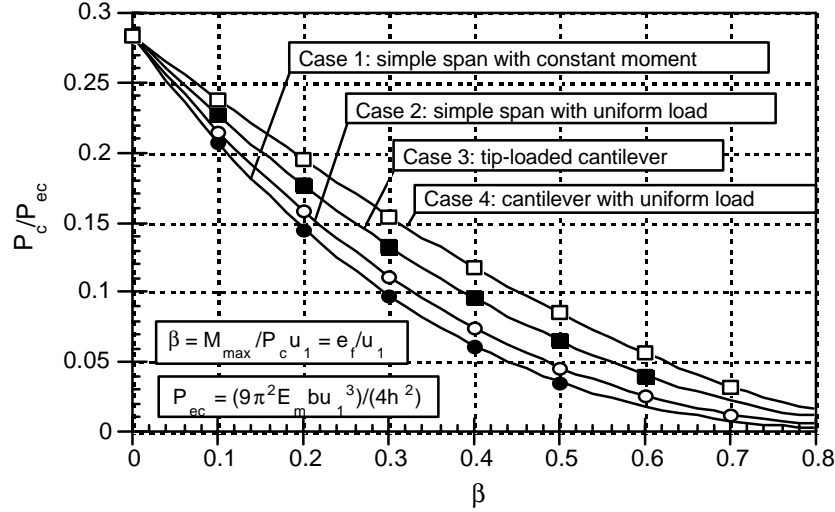


Fig. 3 Influence of bending on buckling capacity of URM walls

Schultz et al. (2000) used the numerical solutions to define the following buckling strength formula on the basis of the MSJC equation for eccentric axial loading (1999)

$$P_c = \frac{\pi^2 E_m I}{h_e^2} \left[1 - 0.577 \left(\frac{e_a + \lambda e_f}{r} \right) \right]^3 \quad [1]$$

where h_e is the effective height kh of an equivalent simply-supported member, and the axial load eccentricity has been replaced by the sum of axial load eccentricity e_a and part of the flexural eccentricity e_f . With values for the constant λ equal to 1.0, 0.905, 0.813, and 0.70, respectively, for Cases 1, 2, 3, and 4, Eq. [1] was found to provide good approximations of the computed buckling strengths.

Bending Moment and Axial Load Interaction

The solutions defined above describe a highly nonlinear interaction between critical axial load P_c and bending moment M_{max} , and are illustrated in Fig. 4 for the load cases considered. Critical axial load and moment are normalized with respect to Euler buckling

load P_E and radius of gyration r . It is noted that for a given moment, there are two values of axial load that produce axial compression instability. One of these is in a branch designated as the “tension” region ($P_c/P_E < 0.4$), for which increases in axial load reduce flexural tension without a comparable increase in $P-\Delta$ instability. The other load is in the remaining branch designated as the “compression” region ($P_c/P_E > 0.4$), for which the reduction in flexural tension does not offset the increased $P-\Delta$ instability.

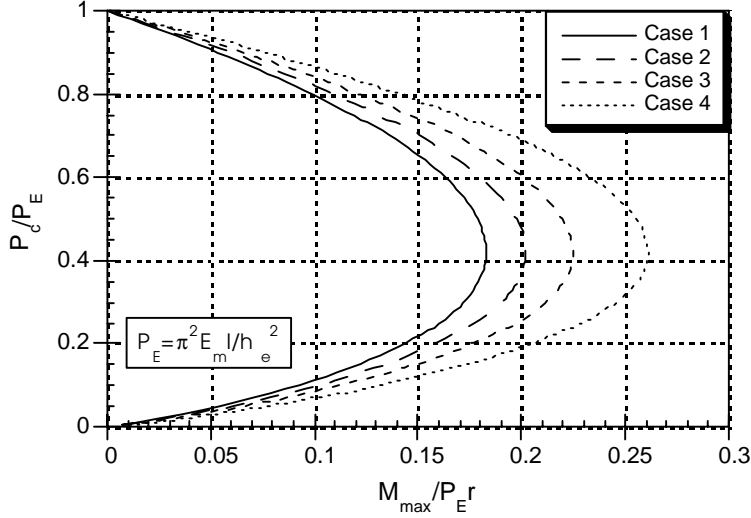


Fig. 4 Moment-buckling load interaction for URM walls

Solution of Eq. [1] for routine design can be cumbersome as it is a fifth-order polynomial. Two different values for axial load satisfy the interaction for a given bending moment, and there is a peak moment for given wall dimensions and material properties beyond which there is no real solution. Rewriting Eq. [1] to solve for maximum moment M_{max} as function of critical load P_c

$$M_{max} = 1.732 \left(\frac{P_c r}{\lambda} \right) \left[1 - 0.577 \left(\frac{e_a}{r} \right) - \sqrt[3]{\frac{P_c}{P_E}} \right] \quad [2]$$

is computationally more expedient than solving Eq. [1].

EXPERIMENTAL PROGRAM

Using the solution for Case 2, the buckling strength of simply-supported, vertically-spanning masonry walls subjected to uniform lateral loads was investigated over a wide range of variables (Schultz and Mueffelman, 2001). Uniform lateral loads at buckling were compared with lateral load capacities for other design criteria including combined axial and flexural compression, flexural tension and out-of-plane horizontal shear. For most parametric combinations considered, the lateral load capacities for buckling were

thick (3 5/8 in.) units. The masonry panels were supported top and bottom by steel beam sections that were attached to pins, the bottom of which were bolted to the laboratory floor. The top pins were the swivel-ended fixtures of two 490 kN (110 kip) force actuators which supplied the axial loading. A single 155-kN (35 kip) horizontal actuator attached to a braced steel column served to provide the horizontal load by means of a whiffletree arrangement comprising threaded steel rods and spreader beams. The whiffletree loaded the masonry panels at four locations along a vertical plane, as shown in Fig. 2, and it produced a lateral moment distribution that simulates closely the moment diagram for uniform lateral pressure. The total height of the specimens between pins was 4.395 m (14 ft 5 in.) and included the steel beams and a portion of the pin fixtures. However, these non-masonry portions of the total pin-to-pin height h were subjected to very small moments, so their influence on behavior was negligible.

At the time this document was written, three of the clay brick walls had been tested. The tests were initiated by applying a pre-selected amount of axial loading to the specimens by means of the vertical actuators, and these loads were subsequently maintained constant. Walls 1, 2 and 3, respectively, sustained axial loads of 111 kN (25 kips), 222 kN (50 kips) and 312 kN (70 kips). The lateral actuator was operated in displacement control, and lateral displacement was incremented slowly until the wall specimens lost all capacity to resist lateral loading. Thus, during the tests, the specimens also resisted second-order ($P-\Delta$) moments generated by the lateral deflection of the masonry. The loading and the specimen response to loading were measured using internal load cells in the actuators, strain gages on the whiffletree rods, and LVDTs at various locations.

TEST RESULTS

The specimens responded to the lateral loading in a controlled manner until the wall cracked. Single horizontal cracks formed near the center of the wall, and the crack widths increased with subsequent loading. Beyond that point, lateral displacement grew quickly and resistance to the lateral load decreased rapidly. The specimens were not allowed to fail in a sudden manner because lateral displacements rather than lateral loads were incremented during the tests, i.e. horizontal actuator displacements were controlled instead of actuator loads. By the end of the tests, even though lateral load capacity of the specimens had been exhausted, second-order ($P-\Delta$) moments were quite large. Plots of the lateral load vs. lateral displacement behavior of the specimens are given in Fig. 6.

By the time Wall 3 was tested, a problem regarding the test setup was discovered. A finite amount of flexural restraint was being imposed by the top and bottom pins of the setup. Thus, Walls 1, 2, and 3 were not tested in a simply-supported configuration, but rather one with flexural restraints at the ends. The lateral displacement profiles for the specimens were used to construct curvature functions, and these functions were searched to identify points of inflection for the specimens. The corresponding locations are reported in Fig. 7 for Walls 2 and 3, but this procedure could not be used for Wall 1 because there were insufficient LVDTs to generate reliable curvature functions. The locations of the points of inflection also served to define the effective height h_e of the specimens, and these are also plotted in Fig. 7.

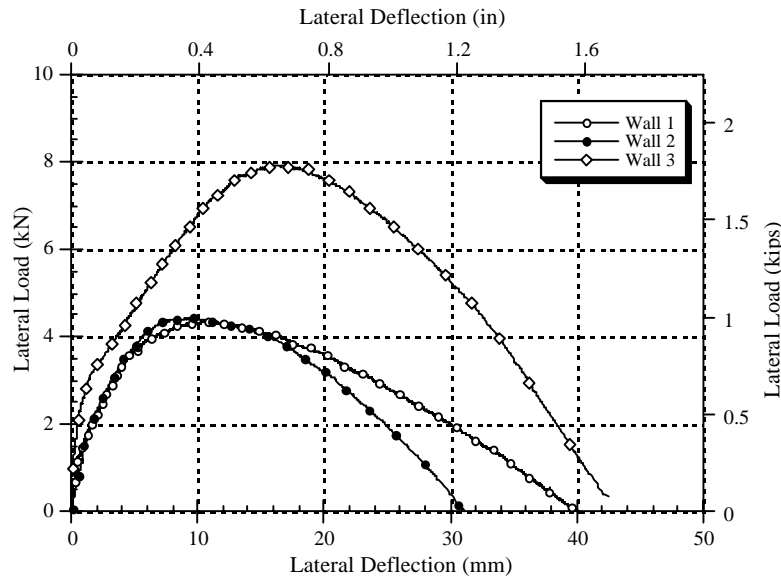


Fig. 6 Lateral load-deflection behavior of brick test walls

The effective heights reported in Fig. 7 are very similar for Walls 2 and 3. By the time the specimens cracked and lost stiffness, bending moment had also peaked, and these instances were taken as the stability limits for the specimens. These occurred at displacements that were roughly equal to 1/3 of the total lateral displacement for Walls 2 and 3. The ratio of effective height h_e to total height h defines effective length factors $k = 0.75$ for Walls 2 and 3. Because no such determination could be made for Wall 1, and since effective heights were so similar for Walls 2 and 3, $k = 0.75$ was also assumed for Wall 1 at the stability limit. Thus, Walls 1, 2 and 3 were much less slender than planned.

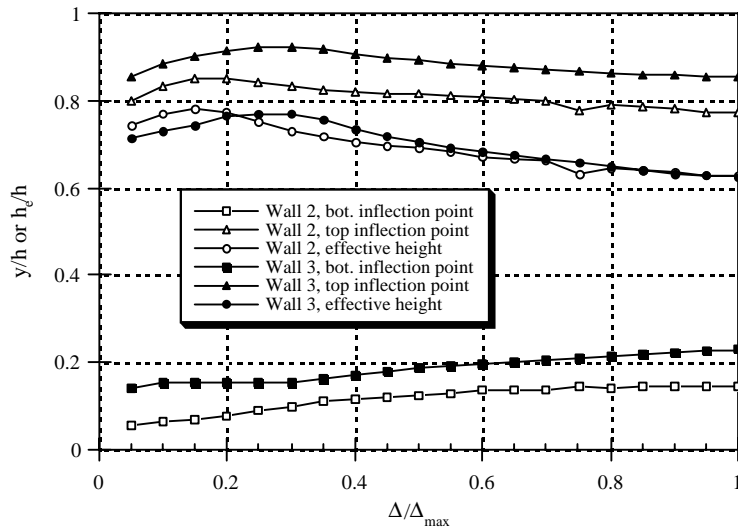


Fig. 7 Points of inflection and effective heights during brick wall tests

Verification of Stability Limits

A bending moment-axial load interaction diagram was constructed using Eq. [2] for an effective height $h_e = kh = 0.75(4.395 \text{ m}) = 3.30 \text{ m}$ (10 ft 10 in.). The diagram is shown in Fig. 8 after normalizing by the Euler buckling load P_E and the radius of gyration r . Data from the tests of Walls 1, 2 and 3 are also indicated. Walls 1 and 3 are seen to approximate the elastic interaction reasonably well, but Wall 2 displayed less bending strength than would be expected from the elastic interaction. This variability can be attributed, in part, to the general variability of masonry material properties. Nonetheless, the tests data is strongly supportive of the stability limits defined by Eq. [1] and [2].

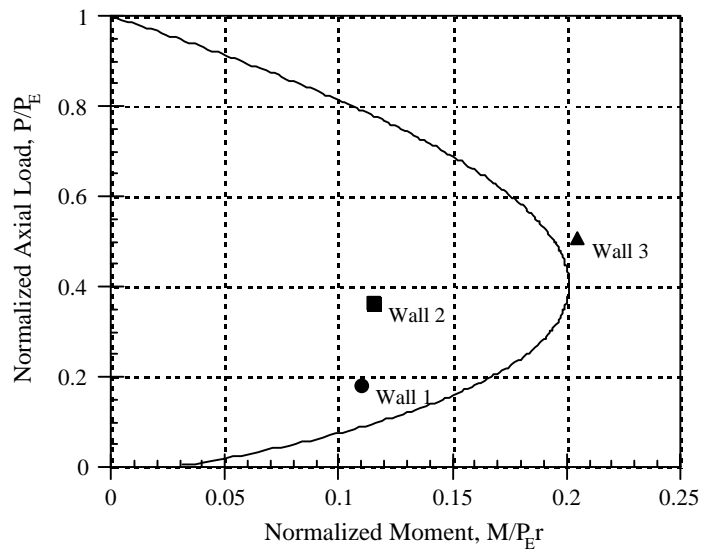


Fig. 8 Verification of moment-axial load interaction for brick walls

The issue of nonlinearity often arises in relation to the stability of URM compression members. Ganduscio (1993) and Romano (1997) reported the buckling solution for a cantilever masonry wall with a concentrated lateral load at the top (i.e., Case 3). They used a nonlinear, exponential stress-strain relation for masonry in compression and noted a marked effect on critical axial loads with increasing degree of nonlinearity. In the U.S., the elastic modulus of masonry E_m is defined as the slope of a line that is secant to the stress-strain curve for masonry in compression at stresses equal to $0.05f'_m$ and $0.33f'_m$, and it incorporates a significant portion of the nonlinearity inherent in masonry behavior. Using E_m defined in this manner, Schultz et al. (2000) demonstrated that the elastic solution represented by Eq. [1] provides a conservative approximation of the nonlinear solution for slender and moderately slender walls ($h/r > 35$). Furthermore, the elastic solution was found to overestimate the nonlinear solution for stocky walls in a substantive manner only when there was little bending (i.e., small β).

As of the writing of this document, the test setup is being modified by replacing the top and bottom pins with commercial bearings so as to reduce the flexural restraint at the ends of the wall specimens. Subsequent tests will be conducted with the modified setup.

CONCLUSIONS

Numerical solutions to the differential equations for flexure of URM members demonstrate 1) deleterious effects on buckling strength with out-of-plane bending, and 2) nonlinear interaction between moment and axial load. However, due to the complexity of this interaction, moment capacity is more expediently defined as a function of axial load at incipient instability rather than the opposite. Nonetheless, the calculations in this and previous studies suggest an urgent need for an experimental investigation of the stability of slender URM walls with transverse loading.

The first three URM specimen tests in a program of 8 walls have been completed. The specimens were tested in a setup that includes constant axial load and monotonically increasing lateral displacement. Under the lateral loading, the wall specimens developed a single crack near mid-height and deflected laterally until all load capacity was exhausted. Problems with the pins in the test setup led to unwanted flexural restraint at the ends of Walls 1, 2 and 3, but specimen displacement data was used to calculate the effective length h_e at the stability limit. The test data strongly suggests the existence of a stability interaction between out-of-plane bending moment and axial load. The test setup is being modified to eliminate the flexural restraint at the ends of the walls, and the remaining 5 specimens will be tested in the new setup.

ACKNOWLEDGEMENTS

This research was conducted with financial support from the National Science Foundation through grant CMS-9904110. Additional support was received from the Minnesota Office of the International Masonry Institute, the Anchor Block Company, and the Minnesota Brick Company. This support is gratefully acknowledged.

REFERENCES

- Angervo, K., *Über die knickung und tragfähigkeit eines excentrisch gedruckten Pfeilers*, Staaliche Technische Forschungsanstalt, Helsinki, 1954.
- Code of Practice for Use of Masonry: Parts 1, 2 and 3*, BS 5628, British Standards Institution, London, 1985.
- Colville, J. , “Stress reduction factors for masonry walls,” *Journal of the Structural Division*, ASCE, 105(ST10):2035-2051, 1979.
- Ganduscio, S., and F. Romano, F, “FEM and analytical solutions for buckling of nonlinear masonry members,” *Journal of Structural Engineering*, ASCE, 123(1):104-111, 1997.
- Masonry Standards Joint Committee, *Building Code Requirements for Masonry Structures*, ACI 530-99/ASCE 5-99/TMS 402-99, American Concrete Institute, Farmington Hills, MI, American Society of Civil Engineers, Reston, VA, The Masonry Society, Boulder, CO, 1999.
- La Mendola, L., M. Papia, and G. Zingone, “Stability of masonry walls subjected to transverse forces,” *Journal of Structural Engineering*, ASCE, 121(11):1581-1587, 1995.
- Minimum Design Loads for Buildings and Other Structures*, ASCE 7-98, American Soc. of Civil Engineers, Reston, VA, 1998, 232 pp.

- NEHRP Recommended Provisions for Seismic Regulations for New Buildings*, 1997 Ed., FEMA 302, Federal Emergency Management Agency. Washington, DC, February 1998.
- Romano, F., S. Ganduscio, and G. Zingone, "Cracked nonlinear masonry stability under vertical and lateral loads," *Journal of Structural Engineering*, ASCE, 119(1):69-87, 1993.
- Sahlin, S., "Transversely loaded compression members made of materials having no tensile strength," *Proceedings*, International Association for Bridge and Structural Engineering, 21:243-253, 1961.
- Schultz, A. E. and Mueffelman, J. G., "Interaction of Bending and Compression in Unreinforced Masonry Members," Department of Civil Engineering, University of Minnesota, Minneapolis, 2001.
- Schultz, A. E., Mueffelman, J. G., and Ojard, N. J., "Critical Axial Loads for Transversely Loaded Masonry Walls" *Proceedings*, 12th International Brick/Block Masonry Conference, Madrid, Spain, June 25-28, 2000.
- Yokel, F. Y., "Stability and capacity of members with no tensile strength," *Journal of the Structural Division*, ASCE, 97(7):1913-1926, 1971.

Notations

- b Section width
- E_m Modulus of elasticity of masonry
- e Eccentricity of axial load
- e_a Actual eccentricity of axial load at end of member
- e_f Effective flexural eccentricity
- f'_m Masonry compression strength
- h Member height
- h_e Effective height of equivalent pin-supported member
- I Moment of inertia of member cross-section about weak axis
- k Effective height factor
- M Bending moment due to out-of-plane lateral load
- M_{max} Maximum bending moment due to out-of-plane lateral load
- P External axial load
- P_E Euler buckling load
- P_{ec} Equivalent critical load based on cracked section depth
- P_c Critical (buckling) load
- r Radius of gyration for member cross-section about weak axis
- t Member thickness
- u Lateral deflection of compression face relative to line of action of axial load
- u_o Maximum lateral deflection of compression face
- u_1 Lateral deflection of compression face at member end
- w Lateral load intensity
- w_u Factored lateral load intensity (at ultimate)
- y Position along wall height
- β Bending parameter (M_{max}/Pu_1)
- D Lateral deflection relative to undeformed configuration
- λ Constant for approximate critical load formula
- σ_o Maximum vertical compression stress in masonry